Available online at www.sciencedirect.com
SCIENCE DIRECT®
Physica C 426–431 (2005) 594–601
PHYSICA C
www.elsevier.com/locate/physc

Approach from temperature measurement to trapped field enhancement in HTSC bulks by pulse field magnetizing

Hiroyuki Fujishiro [a,*], Kazuya Yokoyama [b], Masahiko Kaneyama [a], Manabu Ikebe [a], Tetsuo Oka [c], Koshichi Noto [a,d]

[a] *Faculty of Engineering, Iwate University, 4-3-5 Ueda, Morioka 020-8551, Japan*
[b] *National Institute for Materials Science, 3-13, Sakura, Tsukuba 305-0003, Japan*
[c] *IMRA MATERIAL R & D CO., LTD., 5-50 Hachiken-cho, Kariya 448-0021, Japan*
[d] *Iwate Industrial Promotion Center, 3-35-2 Iiokashinden, Morioka 020-0852, Japan*

Received 23 November 2004; received in revised form 24 January 2005; accepted 24 January 2005
Available online 18 July 2005

Abstract

The time dependences of the temperature rise $\Delta T(t)$ and the magnetization $M(t)$ on the surface of the cryo-cooled SmBaCuO bulk superconductor have been investigated during the five successive magnetic pulse applications (No1–No5) of equal strength ranging from $B_{ex} = 3.83$–6.07 T. The pinning loss (Q_p) is estimated by the hysteresis loss Q^{MH} obtained by the M vs. applied field $\mu_0 H_a$ curve and the viscous loss (Q_v) is estimated by subtracting Q^{MH} from the total Q which is estimated using the maximum temperature rise ΔT_{max} and the specific heat C. For the first pulse (No1) application, Q_p is a main origin of the heat generation and Q_v is dominant for the No5 pulse. The temperature measurements combined with the measurements of the M–$\mu_0 H_a$ curve have been proved to give us the valuable information as for the enhancement of the trapped field by PFM.

PACS: 74.25.Bt; 74.80.Bj; 74.60.Ge

Keywords: Pulse field magnetizing; Heat generation; Pinning and viscous loss; Hysteresis loss

1. Introduction

In view of the applicational use of high-T_c bulk superconductors (HTSCs) as a high-strength bulk magnet for a magnetic separation system to clean up waste water [1] and a magnetron sputtering

* Corresponding author. Tel./fax: +81 19 621 6363.
E-mail address: fujishiro@iwate-u.ac.jp (H. Fujishiro).

0921-4534/$ - see front matter © 2005 Elsevier B.V. All rights reserved.
doi:10.1016/j.physc.2005.05.023

apparatus [2] and so on, the pulse field magnetizing (PFM) have been intensively investigated as well as the static field-cooled magnetizing (FCM) because of the relatively compact, inexpensive and mobile setup. The trapped field B_T^P and total trapped flux Φ_T^P by PFM are, however, generally smaller than those attained by FCM at lower temperatures than 77 K possibly because of the large temperature rise ΔT due to the dynamical motion of the magnetic fluxes against the vortex pinning force F_p and the viscous force F_v. In order to enhance B_T^P and Φ_T^P by PFM, ΔT reduction is an indispensable issue and several approaches such as the iteratively magnetizing pulsed-field method with reducing amplitude (IMRA) [3] and a multi-pulse technique with step-wise cooling (MPSC) [4] have been attempted. We investigated the effect of metal ring setting onto the bulk disk on B_T^P and ΔT [5]. The B_T^P values are 10–20% enhanced by the SUS304 ring because of the heat transfer to the ring.

The heat generation Q during PFM is considered to be the sum of the pinning loss Q_p and the viscous loss Q_v. It is desirable to evaluate the temperature and applied field dependences of the Q_p and Q_v values to understand the PFM mechanism and to attain the optimal B_T^P and Φ_T^P values. Mizutani et al. estimated Q_p and Q_v during PFM using the flux velocity v in the bulk measured by the pick-up coil method [6]. We have studied the time evolution and spatial distribution of the temperature rise $\Delta T(t)$ on the surface of the cryo-cooled YBaCuO [7,8], SmBaCuO [5,9–11] and GdBaCuO [8] bulks during PFM. The $\Delta T(t)$ behavior changed depending on the initial bulk temperature T_s, the strength of the pulse field B_{ex} and the trapped field distribution before the magnetic pulse application. We have estimated the total generated heat Q using the maximum ΔT and the specific heat C of the bulk. Analyzing the pulse number dependence of Q for the five successive pulse applications with the fixed amplitude B_{ex}, the contributions of Q_p and Q_v to the total Q have been roughly separated [10]. Q_p can be estimated from the hysteresis loop of the magnetization M vs. the applied field $\mu_0 H_a$, while Q_v is not directly related with the hysteresis loop. By combining the temperature and magnetic measurements, more precise Q_p and Q_v analyses should become possible.

In this paper, we investigate the time dependences of $\Delta T(t)$ and $M(t)$ for the cryo-cooled SmBaCuO bulk superconductor during the successive magnetic pulse applications with equal strength and estimate the Q_p and Q_v values. We compare the estimated Q_p values by the temperature measurement with those by the M–$\mu_0 H_a$ hysteresis loop. We also discuss the possibility to the B_T^P enhancement on the basis of the temperature measurement data.

2. Experimental

A highly c-axis oriented SmBaCuO bulk superconductor with 45 mm in diameter and 18 mm in thickness was used for measurements, which consisted of four growth sector regions (GSRs) divided by the growth sector boundaries (GSBs). The composition and the detailed fabrication method of the bulk are described elsewhere [12]. The SUS304 ring was set onto the bulk in order to enhance the trapped field by the reduction of the temperature rise [5] and, at the same time, to reinforce the bulk mechanically. The bulk disk was tightly stacked on the sapphire plate attached to the cold stage of a GM-cycle helium refrigerator. The initial stage temperature T_s was fixed at 40 K before every pulse application. The inset of Fig. 1(a) shows the positions on the bulk for the temperature and the trapped field measurements. The time evolution of temperatures, $T0$ at the center of the bulk (P0) and, $T1$–$T4$ at P1–P4 were recorded using fine chromel-constantan thermocouples adhered by GE7031 varnish just after applying the pulse field. P1–P4 were situated on the central radial lines of each GSR by 9 mm apart from P0. The time evolution of the trapped field $B_T^P(t)$ on the bulk surface was measured by the Hall sensor (F.W. Bell, model BHA 921) adhered to the position at PH 2.5 mm distant from P0 using a digital oscilloscope. The total trapped flux Φ_T^P and the distribution of the trapped field $B_T^{3\,mm}$ were measured using an axial-type Hall sensor, which scanned 3 mm above the bulk surface stepwise with a pitch of 1.2 mm. Five iterative magnetic pulses $\mu_0 H_a(t)$ (No1 ~ No5)

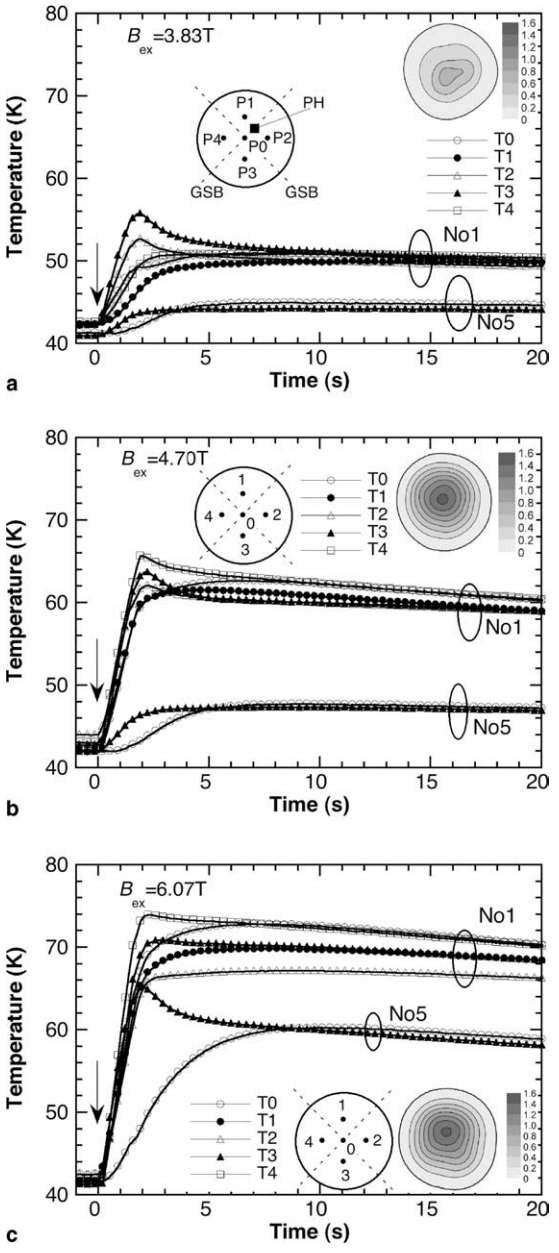

Fig. 1. The time evolutions of $T0(t)$–$T4(t)$ after applying the No1 and No5 pulse fields of: (a) $B_{ex} = 3.83$ T, (b) 4.70 T, (c) 6.07 T, respectively.

with the same maximum amplitude B_{ex} from 3.83 T to 6.07 T (a rise time: $t_p = 12$ ms, a pulse duration: ~100 ms) were applied sequentially after re-cooling the bulk to T_s, where we can obtain the effect of the pure superposition of the pulse field and it is easy to analyze the flux trapping mechanism. B_{ex} was monitored by measuring the current $I(t)$ flowing through the shunt resister.

3. Results and discussion

3.1. Temperature rise and trapped field by iterative PFM

Fig. 1(a)–(c) shows the time evolutions of $T0(t)$–$T4(t)$ on the bulk for $T_s = 40$ K after applying the No1 and No5 pulse fields of (a) $B_{ex} = 3.83$ T, (b) 4.70 T, (c) 6.07 T, respectively. The insets of each figure show the distribution of $B_T^{3\,mm}$ for the No1 pulse. In Fig. 1(a), for the No1 pulse of $B_{ex} =$ 3.83 T, $T2(t)$ and $T3(t)$ rise up first with the maximum temperature rise $\Delta T_{max} = 12$–14 K, followed by $T4(t)$ and $T0(t)$, and $T1(t)$ rises up latest. $T2(t)$ and $T3(t)$ take a maximum at $t = 1.8$ s. But the others slowly increase and then reach a maximum at $t = 5$–10 s. Since the flux motion necessarily generates heat inside the bulk through the mechanisms of Q_p and Q_v, such a rapid temperature rise of *T2* and *T3* suggests the existence of the easy paths for the flux intrusion due to relatively weaker pinning force F_p in GSR2 and GSR3. The distribution $B_T^{3\,mm}$ shows a small peak around P3, which suggests that only the small amount of flux intrudes through the easy path near P3. In Fig. 1(b), for the No1 pulse of $B_{ex} = 4.70$ T, $T2(t)$, $T3(t)$ and $T4(t)$ rise up faster with a peak ($\Delta T_{max} = 20$–24 K), followed by $T1(t)$ and $T0(t)$ rise up latest ($\Delta T_{max} = 19K$). The slow rising up of $T1(t)$ indicates the existence of a hard path for the flux intrusion around P1. The trapped field increases and the distribution takes a cone shape for $B_{ex} = 4.70$ T. In Fig. 1(a) and (b), ΔT_{max} for the No5 pulse decreases and shows no distinct anomaly in $T(t)$. In Fig. 1(c) for the No1 pulse of $B_{ex} = 6.07$ T, ΔT_{max} is as large as 26–34 K and the rise time of $T(t)$ becomes short at all the positions which results from the uniform flux intrusion into the bulk similarly to that in Fig. 1(b) and the cone shape in the $B_T^{3\,mm}$ profile is also maintained. A large and distinct peak in $T3(t)$ can be seen for the No5 pulse, compared with that for

$B_{ex} \leqslant 4.70$ T shown in Fig. 1(a) and (b). This result suggests that the rampant flux motion takes place around P3 even during No5 pulse, supporting again that there is the easiest path near around. In this way, the flux motion can be figured out by monitoring the temperature evolution.

Fig. 2(a) and (b) show the pulse number dependence of the maximum temperature rise ΔT_{max} and the trapped field B_T^P, respectively, for various B_{ex} values. We define $\Delta\ T_{max}$ in Fig. 2(a) as the averaged one from $\Delta T0_{max}$ to $\Delta T4_{max}$. For each B_{ex}, ΔT_{max} is the largest for the No1 pulse and decreases with increasing pulse number, approaching an ultimate value for the No4 and No5 pulses. In Fig. 2(b), a large amount of the magnetic field is trapped by applying the No1 pulse. B_T^P is gradually enhanced with increasing pulse number and then saturates. These saturation tendencies in B_T^P much resemble the behaviors of ΔT_{max} and it can be seen that the flux trapping and temperature rise are closely connected with each other.

Fig. 2(c) summarizes the relation between B_T^P and the maximum temperature $T_{max}(=T_s + \Delta T_{max})$ during PFM on the basis of the results of Fig. 2(a)

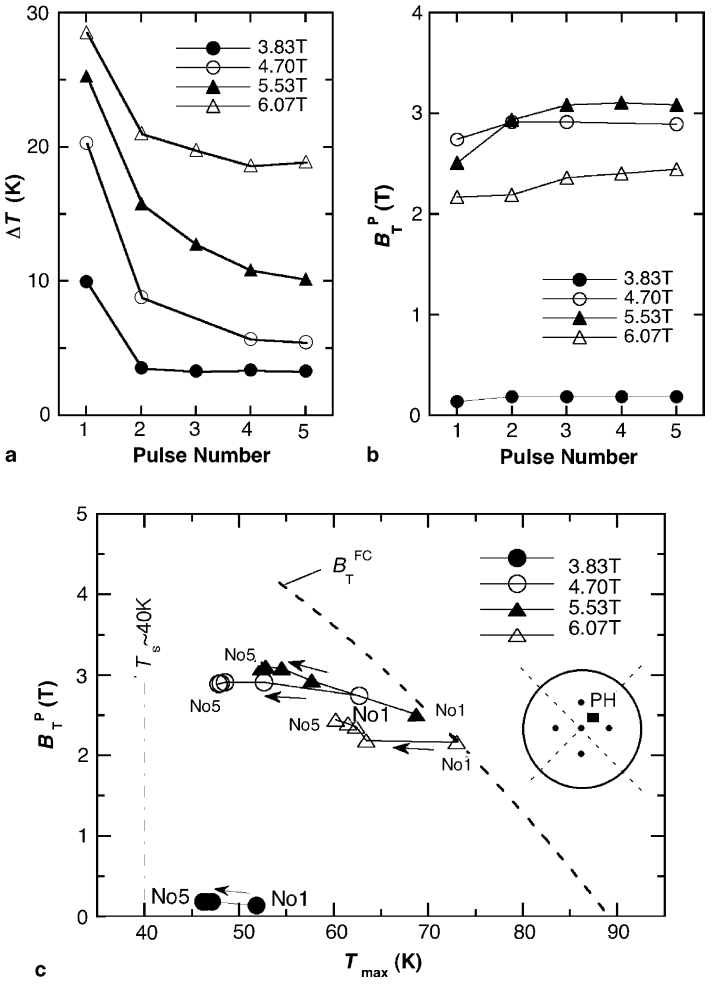

Fig. 2. The pulse number dependence of: (a) the maximum temperature rise ΔT_{max}, (b) the trapped field B_T^P for various B_{ex} = values and (c) the summary of the relation between B_T^P and the maximum temperature $T_{max}(= T_s + \Delta T_{max})$ during PFM. The arrows indicate the change of data sets of (T_{max}, B_T^P) from No1 to No5 pulse for each B_{ex}.

and (b). For each B_{ex} data sets of (T_{max}, B_T^P) from No1 to No5 pulse are plotted. The measured trapped field B_T^{FC} by FCM as a function of T_{max} is also presented, which corresponds to the maximum ability of the flux trapping of this SmBaCuO bulk. The data sets for the No1 pulse of $B_{ex} = 3.83$ T and 4.70 T are situated below the B_T^{FC}–T_{max} line. For the succeeding pulses, T_{max} monotonically decreases and B_T^P slightly increases and then both values saturate for the No5 pulse. For $B_{ex} = 5.53$ T and 6.07 T, the B_T^P value for the No1 pulse is smaller than that for $B_{ex} = 4.70$ T because T_{max} touches the B_T^{FC}–T_{max} line and B_T^P decreases following the line with the further increase of temperature. After the succeeding pulse application, B_T^P increases with increasing pulse number and the highest value of 3.09 T can be obtained for the No5 pulse of $B_{ex} = 5.53$ T. These analyses demonstrate that the flux trapping ability by the PFM technique can be systematically explained as limited by the B_T^{FC}–T_{max} line.

3.2. Estimation of pinning loss Q_p and viscous loss Q_v based on the temperature measurement

In order to elucidate the magnetizing mechanism by PFM and to enhance B_T^P, it is important to know the generated heat Q, because Q contains more exact information than ΔT indispensable for detailed analyses. If we assume that the heat generation occurs under the adiabatic condition, the Q value is represented by the following equation [10]:

$$Q = \int_{T_s}^{T_s+\Delta T_{max}} C(T) V \, dT = Q_P + Q_V, \quad (1)$$

where $C(T)$ is the specific heat and V is the volume of the bulk disk. $C(T)$ was estimated using the relation $C = \mathscr{K}/\alpha$, i.e., the thermal conductivity $\mathscr{K}$ divided by the thermal diffusivity α, both of which were measured simultaneously [13,14].

Fig. 3 presents the estimated Q(No1) and Q(No5) values after the No1 and No5 pulse together with the difference $dQ(= Q(\text{No1}) - Q(\text{No5}))$ as a function of B_{ex}. The inset displays $C(t)$ of the SmBaCuO bulk. Both Q(No1) and Q(No5) increase with increasing B_{ex}. However, the Q(No1)–B_{ex} curve is convex and the Q(No5)–B_{ex} curve is concave. The heat generation during

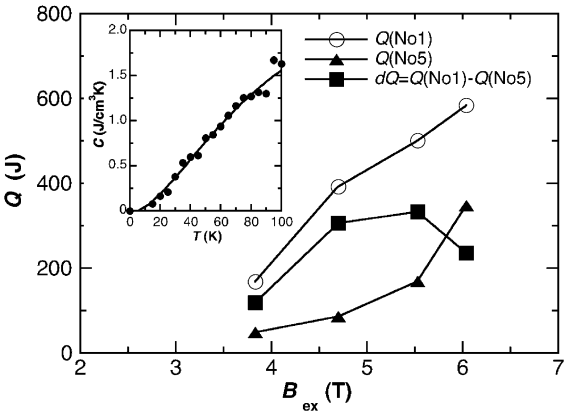

Fig. 3. The estimated Q(No1) and Q(No5) values after the No1 and No5 pulse and the difference dQ (=Q(No1)-Q(No5)) as a function of B_{ex}. The specific heat $C(T)$ of the SmBaCuO bulk used in this study is also shown in the inset.

PFM is given by the sum of Q_p and Q_v as presented by Eq. (1) and flux trapping should be closely connected with Q_p. Since no additional flux trapping takes place for the No5 pulse, it is reasonable to assume that the difference dQ roughly stands for the pinning loss connected to the flux trapping for the No1 pulse. Then Q(No5) may mainly consists of Q_v.

3.3. Determination of pinning loss Q_p using M–$\mu_0 H_a$ curve

Following the idea of the critical state model, Q_p can be qualitatively divided into two components, Q_p^T and Q_p^L, as schematically illustrated on a hypothetical M–$\mu_0 H_a$ hysteresis loop for quasi-static magnetizing in Fig. 4,

$$Q_P = Q_P^T + Q_P^L, \quad (2)$$

where Q_p^T is the pinning loss inevitable for the flux trapping, while Q_p^L is additional pining loss unrelated with the flux trapping. In Fig. 4, it is anticipated that there is a threshold applied field $\mu_0 H_{th}$ which provides the boundary between Q_p^T and Q_p^L on the M–$\mu_0 H_a$ space. We have measured the time dependence of the applied field $\mu_0 H_a(t)$ and the trapped field $B(t)$. The magnetization M in the bulk is given by

$$M = B - \mu_0 H_a. \quad (3)$$

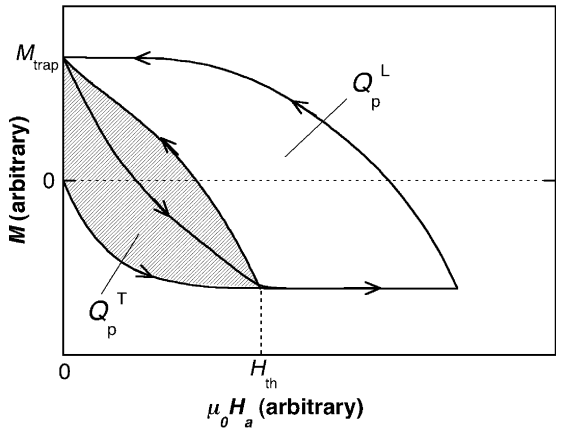

Fig. 4. The schematic view of the hypothetical M–$\mu_0 H_a$ hysteresis loop during quasi-static magnetizing. The hysteresis loss Q_p can be qualitatively divided into two components, $Q_p^T$and Q_p^L (see text). The hysteresis loop starting from M_{trap} corresponds to the second run.

Fig. 5 shows the M vs. $\mu_0 H_a$ curves for the No1, No2 and No5 pulses of $B_{ex} = 3.83$–6.02 T. In Fig. 5(a), for $B_{ex} = 3.83$ T, the magnetic fluxes can hardly penetrate into the bulk center and the M value is nearly equal to the applied field $\mu_0 H_a (M \sim -\mu_0 H_a)$ and the hysteresis behavior cannot be observed. In Fig. 5(b) and (c) for $B_{ex} = 4.70$ T and 5.53 T, a wide hysteresis loop in M–$\mu_0 H_a$ curve can be clearly seen for the No1 pulse which may mainly result from the flux trapping by the bulk disk. The hysteresis loop is slightly enhanced with increasing B_{ex}. For the No2 pulse, the hysteresis loop becomes drastically narrow and no hysteresis behavior can be observed for the No5 pulse. In contrast, the pulse number dependence of the M–$\mu_0 H_a$ curve of for $B_{ex} = 6.07$ T in Fig. 5(d) is somewhat different; a sizable hysteresis remains even for the No5 pulse. Since the trapped flux is not enhanced for the No5 pulse of $B_{ex} = 6.07$ T, the hysteresis loss for the No5 pulse is attributable to Q_p^L.

Fig. 6(a) shows the pulse number dependence of the Q^{MH} values determined from the M–$\mu_0 H_a$ hysteresis loop for each B_{ex}. For $B_{ex} = 3.83$ T, Q^{MH} is negligibly small because of no observable hysteretic behavior. For $B_{ex} = 4.70$ T and 5.53 T, the Q^{MH} value for the No1 pulse is the largest and suddenly decreases after the No2 pulses and then approaches to zero. For $B_{ex} = 6.07$ T, Q^{MH} decreases with increasing pulse number, but the finite Q^{MH} value of ~150 J exists even for the No5 pulse. Fig. 6(b) displays the increment of the total trapped flux $d\Phi_T^P = \Phi_T^P(\text{No } i) - \Phi_T^P(\text{No } i-1)$ as a function of the pulse number i. For the first pulse ($i = 1$), $d\Phi_T^P$ is defined as Φ_T^P (No1). The behaviors of $d\Phi_T^P$ or the increment of the B_T^P value in Fig. 2(b) are much similar to Q^{MH} shown in Fig. 6(a), except for the Q_p^L contribution which shows the offset for $B_{ex} = 6.07$ T.

Fig. 7(a) and (b) present the total heat generation Q determined from the temperature measurement, Q^{MH} and the difference $\Delta Q = Q$–Q^{MH} for the No1 and No5 pulses, respectively, as a function of B_{ex}. In Fig. 7(a), ΔQ is equal to the viscous loss Q_v(No1) because $Q^{MH} = Q_p$. However, for $B_{ex} = 3.83$ T, the estimated Q_p(No1) = 0 should

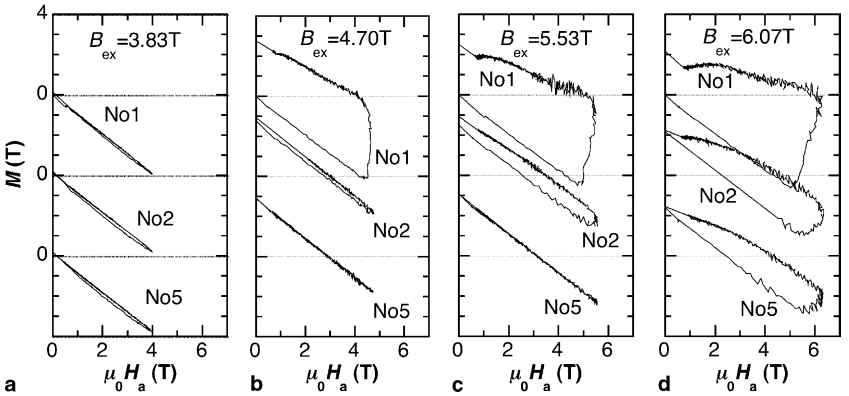

Fig. 5. The measured M–$\mu_0 H_a$ curves for the No1, No2 and No5 pulses of $B_{ex} = 3.83$–6.02 T.

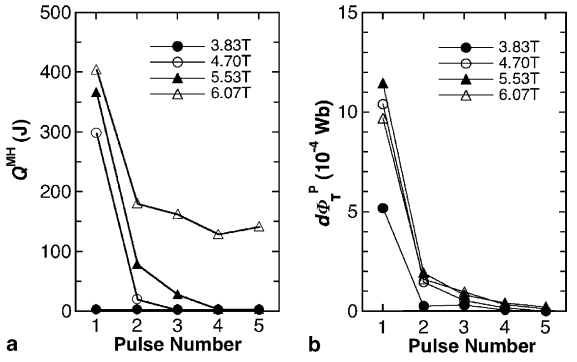

Fig. 6. (a) The pulse number dependence of Q^{MH} determined from the M–$\mu_0 H_a$ loop. (b) The increment of the total trapped flux $d\Phi_T^P = \Phi_T^P(\text{No } i) - \Phi_T^P(\text{No } i-1)$ as a function of pulse number.

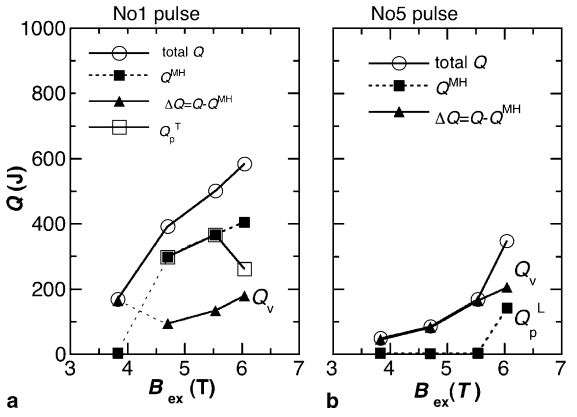

Fig. 7. Total Q, Q^{MH} and the difference $\Delta Q = Q - Q^{MH}$ as a function of B_{ex} for the (a) No1 and (b) No5 pulses. The Q_p^T, Q_p^L and Q_v values are estimated for each pulse (see text).

be underestimated because a sizable amount of magnetic flux is actually trapped as is seen in Fig. 6(b) in spite of apparent non-hysteresis behavior of the M–$\mu_0 H_a$ curve. Because the position PH, which is defined in the inset in Fig. 1(a), is located near the hard path around P1, the measuring position dependence of $M(t)$ should be taken account of. It is also to be noticed that Q_v(No1) is represented by nearly a linear function of B_{ex} as a whole. In this figure, Q^{MH}(No1) can be regarded as the trapping pinning loss Q_p^T(No1) except for $B_{ex} = 6.07$ T because of the absence of the hysteresis loss Q^{MH}(No5) for the No5 pulse below $B_{ex} = 5.53$ T shown in Fig. 7(b).

For the No5 pulse shown in Fig. 7(b), because of the absence of Q^{MH}(No5), our previous assumption [10] that Q(No5) = Q_v may be acceptable for $B_{ex} \leqslant 5.53$ T. For $B_{ex} = 6.07$ T, Q_v(No5) is estimated by the relation of Q_v(No5) = Q(No5)–Q^{MH}(No5) and B_{ex} dependence of Q_v(No5) again falls on a nearly linear function. It is clear that the Q(No5)–B_{ex} concave curve originates from the appearance of Q^{MH} for $B_{ex} = 6.07$ T. We also notice that Q^{MH}(No5) for $B_{ex} = 6.07$ T corresponds to Q_p^L notlinked with the flux trapping. Since Q_p^L of this size is considered to be also contained in Q^{MH}(No1), this Q_p^L must be subtracted from Q^{MH}(No1) to estimate the trapping loss Q_p^T(No1) for $B_{ex} = 6.07$ T as shown in Fig. 7(a). The Q_p^T(No1) value for $B_{ex} = 6.07$ T is smaller than those for $B_{ex} = 4.70$ T and 5.53 T because of the smaller amount of the trapped flux.

4. Summary

The time dependences of the temperature rise $\Delta T(t)$ and the magnetization $M(t)$ on the surface of the cryo-cooled SmBaCuO bulk superconductor have been investigated during the identical magnetic pulse successive applications (No1–No5) from $B_{ex} = 3.83$–6.07 T. Main experimental results and conclusions obtained in this study are summarized as follows.

(1) The simultaneous temperature $T(t)$ and magnetization $M(t)$ measurements during pulse field magnetizing enable us to separate the generated heat due to the flux pinning loss Q_p and the viscous loss Q_v more precisely.
(2) For the No1 pulse application to the virgin state bulk, the pinning loss Q_p determined from the M vs. applied field $\mu_0 H_a$ curve is the main origin of the heat generation and Q_v, which is estimated by the subtraction of Q^{MH} from the total Q, is the dominant origin for the No5 pulse.
(3) There is a threshold field $B_{th} = \mu_0 H_{th}$ above which the pinning loss Q_p^L unrelated to the flux pinning increases rapidly. B_{th} is located just above $B_{ex} = 5.53$ T for the present SmBaCuO bulk with 45 mm in diameter.

(4) The spatial dependence of $\Delta T(t)$ enable us to locate the easy paths and the hard path for the flux intrusion and it is found that the temperature measurements combined with the measurement of the M–$\mu_0 H_a$ curve give us valuable information in order to enhance the trapped field by PFM.

Acknowledgements

This work is partially supported by Japan Science and Technology Corporation under the Joint-research Project for Regional Intensive in the Iwate Prefecture on "Development of practical applications of magnetic field technology for use in the region and in everyday living".

References

[1] H. Hayashi, K. Tsutsumi, N. Saho, N. Nishijima, K. Asano, Phys. C 392–396 (2003) 745.
[2] U. Mizutani, H. Hazama, T. Matsuda, Y. Yanagi, Y. Itoh, K. Sakurai, A. Imai, Supercond. Sci. Technol. 16 (2003) 1207.
[3] U. Mizutani, T. Oka, Y. Itoh, Y. Yanagi, M. Yoshikawa, H. Ikuta, Appl. Supercond. 6 (1998) 235.
[4] M. Sander, U. Sutter, R. Koch, M. Kläser, Supercond. Sci. Technol. 13 (2000) 841.
[5] H. Fujishiro, T. Oka, K. Yokoyama, M. Kaneyama, K. Noto, IEEE Trans. Appl. Supercond. 14 (2004) 1054.
[6] U. Mizutani, H. Ikuta, T. Hosokawa, H. Ishihara, K. Tazoe, T. Oka, Y. Itoh, Y. Yanagi, M. Yoshikawa, Advances in Superconductivity XII, Springer-Verlag, Tokyo, 2000, pp. 431–436.
[7] H. Fujishiro, T. Oka, K. Yokoyama, K. Noto, Supercond. Sci. Technol. 16 (2003) 809.
[8] H. Fujishiro, M. Kaneyama, K. Yokoyama, T. Oka, K. Noto, Supercond. Sci. Technol. 18 (2005) 158.
[9] H. Fujishiro, K. Yokoyama, T. Oka, K. Noto, Supercond. Sci. Technol. 17 (2004) 51.
[10] H. Fujishiro, K. Yokoyama, M. Kaneyama, T. Oka, K. Noto, Physica C 412–414 (2004) 646.
[11] K. Yokoyama, M. Kaneyama, T. Oka, H. Fujishiro, K. Noto, Physica C 412–414 (2004) 688.
[12] S. Kohayashi, H. Miyairi, S. Yoshizawa, S. Haseyama, S. Nagaya, H. Nakane, Physica C 357–360 (2001) 789.
[13] M. Ikebe, H. Fujishiro, T. Naito, K. Noto, J. Phys. Soc. Jpn. 63 (1994) 3107.
[14] H. Fujishiro, S. Kohayashi, IEEE Trans. Appl. Supercond. 12 (2002) 1124.